Optical Engineering

SPIEDigitalLibrary.org/oe

Adjustable-window grating interferometer based on a Mach-Zehnder configuration for phase profile measurements of transparent samples

David-Ignacio Serrano-García
Noel-Ivan Toto-Arellano
Amalia Martínez-García
Juan-Antonio Rayas-Álvarez
Gustavo Rodríguez-Zurita
Areli Montes-Pérez

SPIE

Adjustable-window grating interferometer based on a Mach-Zehnder configuration for phase profile measurements of transparent samples

David-Ignacio Serrano-García
Centro de Investigaciones en Óptica A.C.
León, Gto
México
E-mail: david@cio.mx

Noel-Ivan Toto-Arellano
Universidad Tecnológica de Tulancingo
Departamento de Óptica y Fotónica
Tulancingo, Hidalgo
México
and
Benemerita Universidad Autónoma de Puebla
Laboratorio de Óptica Física de la Facultad de Ciencias Físico-Matemáticas
Puebla, Pue
México
E-mail: ivantotoarellano@hotmail.com

Amalia Martínez-García
Juan-Antonio Rayas-Álvarez
Centro de Investigaciones en Óptica A.C.
León, Gto
México

Gustavo Rodríguez-Zurita
Areli Montes-Pérez
Benemerita Universidad Autónoma de Puebla
Laboratorio de Óptica Física de la Facultad de Ciencias Físico-Matemáticas
Puebla, Pue
México

Abstract. This communication describes some details of polarization modulation that are useful in phase-shifting interferometry when applied to phase profile measurements of phase objects. Since non-destructive optical techniques allow surface measurement with high accuracy, a Mach-Zehnder configuration coupled to a 4-*f* arrangement using phase gratings placed on the Fourier plane was implemented to analyze phase objects. Each beam of the interferometer goes through a birefringent wave plate in order to achieve nearly circular polarization of opposite rotations, with respect to each other. The interference of the fields associated with replicated beams, centered on each diffraction order, is achieved varying the spacing of windows with respect to the grating period. Experimental results are presented for cases of four and nine simultaneously captured interferograms. [DOI: 10.1117/1.OE.51.5.055601]

Subject terms: phase shifting; interferometry; phase objects; phase grating.

Paper 111231 received Oct. 3, 2011; revised manuscript received Mar. 10, 2012; accepted for publication Mar. 13, 2012; published online May 4, 2012.

1 Introduction

In this work, we propose a configuration of a two-window polarizing phase shifting interferometer,[1,2] based on two coupled systems: a Mach-Zehnder interferometer (MZI) that allows the two-window generation with adjustable separation, and a 4-*f* system with Phase gratings placed on the frequency plane;[3,4] due to that, the change in beam separation can be freely adjusted. One advantage is that, when beam separation is properly changed, interference of the different diffractions orders can be obtained. The system is insensitive to external vibrations itself due to its quasi-common path configuration. The previously presented two-window interferometer with diffraction grating[3] was implemented using a fixed separation exclusively designed for the grid used; in the proposed configuration, we can freely adjust these separation and positions. Also, with the proposed optical system, we can obtain results of the same quality as those obtained in previous reports, in a more flexible system which is not limited by optical components, such as the grid used. The MZI system, unlike a system based on a Sagnac triangular, has the advantage of being adapted for use in other applications, such as microscopy (placing a microscopic system on one arm) or phase shifting optical tomography (by obtaining parallel projections for each angle of rotation of the transparent sample); the aforementioned applications are considered future work of the research proposed in this report.

To generate independent phase shifts in the interference patterns, a linear polarizer is placed at a convenient angle on each replica.[5] In the experimental results presented, the Interference patterns are processed by means of two methods, for the case of four interferograms and in the case of nine interferograms, using the symmetrical $(N+1)$ nine algorithms.[6,7]

2 Experimental Setup

The optical system proposed is shown in Fig. 1. It consists of a combination of a quarter-wave plate Q and a linear polarizing filter P_0 that generates linearly polarized light oriented

0091-3286/2012/$25.00 © 2012 SPIE

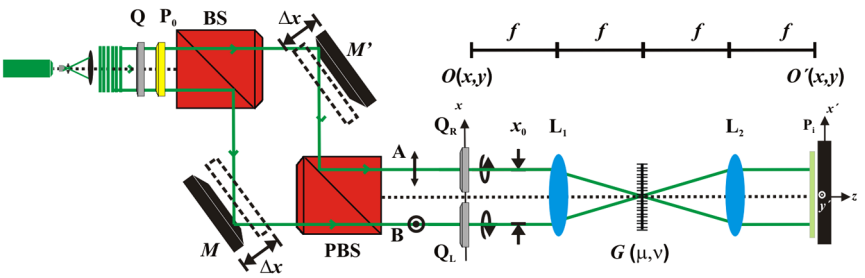

Fig. 1 Experimental setup. BS: Beamsplitter PBS: polarizing beamsplitter $O(x, y)$: object plane $O'(x, y)$: image plane L_i: lens $G(\mu, v)$: phase grid P_i: polarizer's grating period $d = 110$ lines/mm $x_0 = 10$ mm$f = 150$ mm$\alpha' = 1.519$ rad. The transparent sample is collocated on B.

at a 45-deg angle entering the Mach Zehnder configuration from a YVO_3 laser operating at 532 nm (see Fig. 1). This configuration generates two symmetrically displaced beams by moving mirrors M and M' enabling one to change spacing x_0 between beam centers. Two retardation plates (Q_L and Q_R), with mutually orthogonal fast axes, are placed in front of the two beams (A, B) to generate left and r ight nearly-circular polarized light.[8,9] A phase-grating $G(u/\lambda f, v/\lambda f)$ is placed on the frequency plane (u, v) of the 4-f Fourier optical system that is coupled to the MZI configuration, with f being the focal length of each transforming lens. Then, $\mu = u/\lambda f$ and $\upsilon = v/\lambda f$ are the frequency coordinates scaled to wavelength λ and the focal length. On plane (μ, υ), the period of G is denoted by d, and its spatial frequency by $\sigma = 1/d$. Two neighboring diffraction orders have a distance of $X_0 \equiv \lambda f/d$ at the image plane for a grating; then, $\sigma \cdot u = X_0 \cdot \mu$ and X_0 can be used as a frequency. In the following sections, phase shifts caused by the grating at the image plane of this system are discussed.

3 Phase Grating Interferometry

Phase gratings have interesting properties, as well as the advantage of using a higher percentage of incident energy than absorption gratings. In this report, we use cross-phase gratings, with the advantage of being able to generate up to 16 replicas of the interferogram with independent phase shifts; this allows the use of other algorithms to process phase. Furthermore, the use of cross-phase gratings allows one to obtain π-phase shifts, simplifying the polarizer arrangement. It is known from Ref. 10 that the retardation error generated by the wave plates and the phase aberration of the diffractive elements can be neglected, the intensity aberration of diffractive wavefronts, and pixel mismatch should be corrected.[10] One should select good optical elements, such as high efficiency gratings, imaging lens and detectors. A phase grid, carefully constructed by means of superposing two phase gratings with their respective grating vectors at ± 90 deg, is placed at the system's Fourier planes. Taking the rulings of one grating along the $\mu = u/\lambda f$ direction and the rulings of the second grating along the $\upsilon = v/\lambda f$ direction, the resulting centered phase grid can be written as

$$G(\mu, \upsilon) = e^{i2\pi A_g \sin[2\pi \cdot X_0 \mu]} e^{i2\pi A_g \sin[2\pi \cdot X_0 \upsilon]} = \sum_{q=-\infty}^{\infty} J_q(2\pi A_g) e^{i2\pi \cdot qX_0 \mu} \sum_{r=-\infty}^{\infty} J_r(2\pi A_g) e^{i2\pi \cdot rX_0 \upsilon}, \quad (1)$$

where the frequencies along each axis direction are taken as X_0, with 2πAg being the phase grating amplitude, and J_q and J_r the Bessel functions of the first kind of integer order q, r, respectively. The Fourier transform of the phase grid becomes

$$\tilde{G}(x, y) = \sum_{q=-\infty}^{q=\infty} \sum_{r=-\infty}^{r=\infty} J_q(2\pi A_g) J_r(2\pi A_g) \delta(x - qX_0, y - rX_0), \quad (2)$$

which consists of point-like diffraction orders distributed on the image plane.

3.1 *Interference-Pattern Contrasts and Modulation*

Phase grid interferometry is based on a two crossed phase grating placed as the pupil in a 4-f Fourier optical system. A convenient window pair for a grating interferometer implies an amplitude transmittance given by

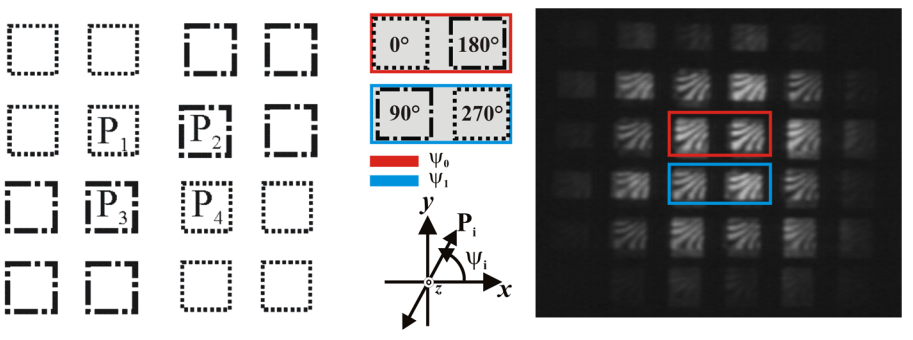

(a) (b)

Fig. 2 Replicas of the interference patterns obtained with the phase grid. (a) Polarizing filters array and (b) experimental interference patterns.

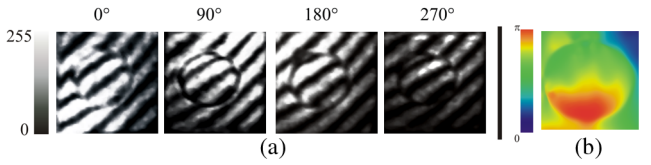

Fig. 3 Phase dot prepared evaporating magnesium fluoride (MgF_2) on a glass substrate. (a) Four 90 deg phase-shifted interferograms and (b) phase profile.

$$O(x,y) = A\left(x + \frac{x_0}{2}, y\right) + B\left(x - \frac{x_0}{2}, y\right), \tag{3}$$

where x_0 is the separation from center to center between two beams, $A(x,y)$ as the reference beam aperture and $B(x,y)$ is the beam aperture where the phase object is placed. Placing a grating of spatial period $d = \lambda f / F_0$ at the Fourier plane, with a corresponding transmittance given by $G(\mu, \upsilon)$. The image formed by the system consists basically of replications of each window at distances F_0. This image is defined by $O'(x,y)$; that is, the convolution of $O(x,y)$ with the Fourier transform of the phase grating, $\tilde{G}(x,y)$ represented by

$$\begin{aligned} O'(x,y) &= O(x,y) * \tilde{G}(x,y) \\ &= w\left(x + \frac{x_0}{2}, y\right) * \sum_{q=-\infty}^{\infty} J_q(2\pi A_g)\delta(x - qF_0, y) \\ &\quad + \left[w\left(x - \frac{x_0}{2}, y\right) e^{i\phi\left(x - \frac{x_0}{2}, y\right)}\right] \\ &\quad * \sum_{q=-\infty}^{\infty} J_q(2\pi A_g)\delta(x - qF_0, y), \end{aligned} \tag{4}$$

where (*) denotes the convolution. By adding the terms of Eq. (4), taking q and $q-1$ (both located within the same replicated window $w(x - qF_0 + \frac{x_0}{2}, y)$), and for the case of matching the beams's positions with the diffraction order's positions ($F_0 = x_0$), the previous equation simplifies to

$$\begin{aligned} O'(x,y) = \sum_{q=-\infty}^{\infty} &\left[J_q(2\pi A_g) + J_{q-1}(2\pi A_g) e^{i\phi(x - x_0[q - \frac{1}{2}], y)}\right] \\ &w\left[x - x_0\left(q - \frac{1}{2}\right), y\right]. \end{aligned} \tag{5}$$

Thus, an interference pattern between fields associated to each window must appear within each replicated window. The fringe modulation m_q of each pattern would be of the form

$$m_q = \frac{2J_q J_{q-1}}{J_q^2 + J_{q-1}^2}, \tag{6}$$

where each fringe contrast depends on the relative phases between the Bessel functions J_q.

3.2 *Phase Shifting Interferometry with Modulation of Polarization*

Turning the attention to gratings, in order to introduce additional phase shifts in the interference pattern centered around $(x_0[q - (1/2)], y)$, each of the windows is illuminated with different polarizations using retarding plates Q_R and Q_L (Fig. 1); this arrangement introduces Jones polarization vectors $\vec{J}_R$ and $\vec{J}_L$ into the interference terms of Eq. (4). After placing a linear polarizing filter with the transmission axis at an angle ψ, its irradiance turns out to be proportional to

$$\begin{aligned} \|\vec{J}_T\|^2 = A(\xi, \alpha')\{&(J_q^2 + J_{q-1}^2) \\ &+ 2J_q J_{q-1} \cos[\xi(\psi, \alpha') - \phi(x,y)]\}, \end{aligned} \tag{7}$$

where $\vec{J}_T = J_\psi^l \vec{J}_L J_q + J_\psi^l \vec{J}_R J_{q-1}$, J_ψ^l is the transmission matrix for the linear polarizer at angle ψ, $\pm\alpha'$ is the retardation of each plate, and $\xi(\psi, \alpha')$ denotes the phase shifting term induced by modulation of polarization given by

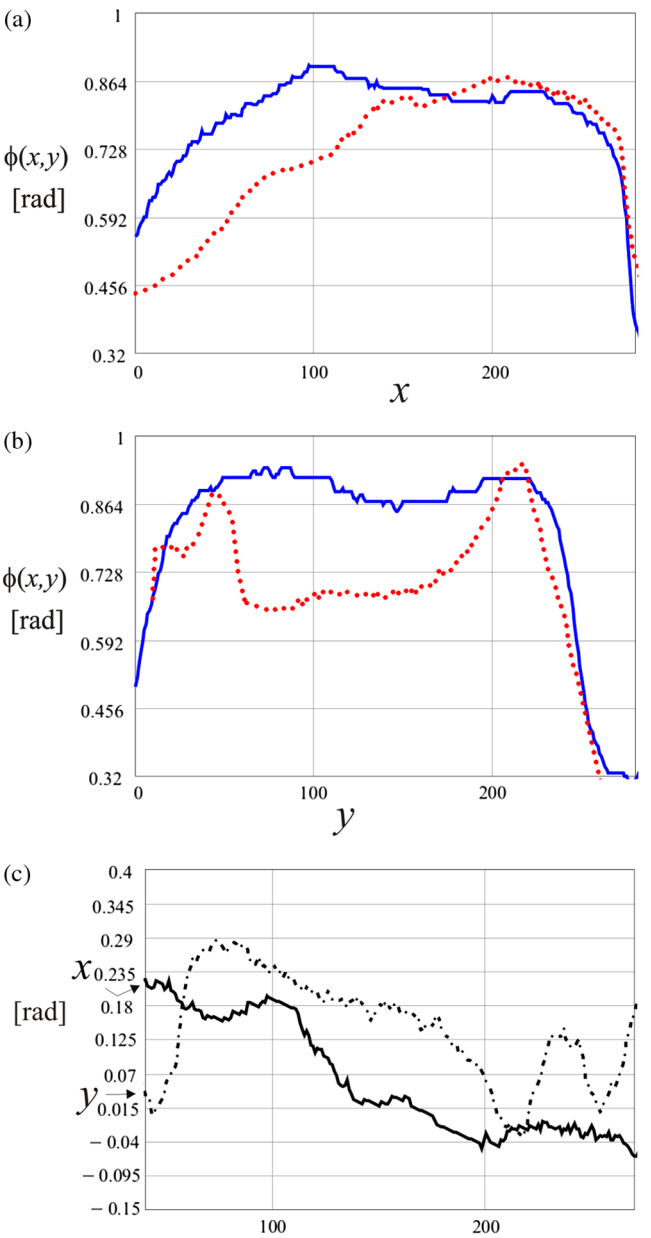

Fig. 4 Continued line: Phases along typical raster lines of phase dot of Fig. 3; Dotted line: Phases along typical raster lines of phase dot of Ref. 1; (a) Traze along-x, (b) traze along-y, and (c) plot of differences along the two directions.

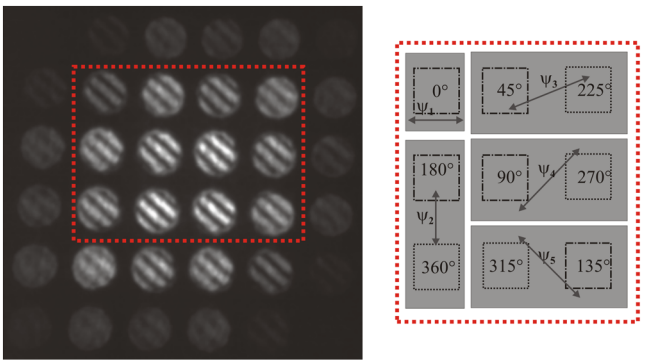

(a) (b)

Fig. 5 Interference patterns detected with a polarizing filter at $\psi = 25$ deg. (a) The interference patterns used are enclosed in the dotted rectangle and (b) polarizer filter array for $N = 8$, nine symmetrical interferograms.

$$\xi(\psi,\alpha') = \mathrm{Arc\,Tan}\left[\frac{\sin[2\psi]\cdot\sin[\alpha'] + \sin^2[\psi]\cdot\sin[2\alpha']}{\cos^2[\psi] + \sin^2[\psi]\cdot\cos[2\alpha'] + \sin[2\psi]\cdot\cos[\alpha']}\right]; \tag{8}$$

$A(\psi,\alpha')$ is defined as

$$A(\psi,\alpha') = 1 + \sin[2\psi]\cos[\alpha'] \tag{9}$$

denoting each pattern as

$$\|\vec{J}_i\|^2 = A(\xi,\alpha')\{(J_q^2 + J_{q-1}^2) + 2J_qJ_{q-1}\cos[\xi(\psi_i,\alpha') - \phi(x,y)]\} \tag{10}$$

with $i = 1 \ldots N$.

3.2.1 *Case of four interferograms*

For phase-shifting interferometry with four patterns, four irradiances can be used, each one taken at a different ψ angle. The relative phase can be calculated by Refs. 6 and 11

$$\tan\phi = \frac{\|\vec{J}_1\|^2 - \|\vec{J}_3\|^2}{\|\vec{J}_2\|^2 - \|\vec{J}_4\|^2}, \tag{11}$$

where $\|\vec{J}_1\|^2$, $\|\vec{J}_2\|^2$, $\|\vec{J}_3\|^2$ and $\|\vec{J}_4\|^2$ are the intensity measurements with the values of ψ such that $\xi(\psi_1) = 0$, $\xi(\psi_2) = \pi/2$, $\xi(\psi_3) = \pi$, $\xi(\psi_4) = 3\pi/2$, respectively. Note that $\xi(\psi,\pi/2) = 2\psi$ and $A(\psi,\pi/2) = 1$, so a good choice for the retarders is quarter-wave retarders, as it is well known. Dependence of ϕ on the coordinates of the centered point has been simplified to x, y. The same fringe modulation m_q results as in Eq. (6). Therefore, the discussion about fringe modulation given in previous sections is retained when introducing the modulation of polarization. Such polarization modulation can be carried out also for grids, resulting in similar conclusions.

3.2.2 *Case of nine interferograms*

To demonstrate the use of the various interferograms obtained to extract phase under the conditions described above, we choose the symmetrical $N + 1$ phase steps algorithms for data processing, the phase is given by Ref. 7:

$$\tan\phi(x,y) = \frac{\sum_i^{N+1} I_i \sin\left(2\pi\frac{i-1}{N}\right)}{\sum_i^{N+1} I_i \cos\left(2\pi\frac{i-1}{N}\right)}, \tag{12}$$

where $N + 1$ is the number of interferograms. For the case of nine interferograms, only five linear polarizing filters have to be placed. The transmission axes of the filter pairs P_1 can be the same for each one, as long as they cover two patterns with π-phase shift in between.

3.3 *Phase Shifts*

Experimentally, the phase shifting obtained is the result of placing a linear polarizer in each one of the interference patterns generated on each diffracting orders on the exit plane (P_i); each polarizing filter transmission axis is adjusted at a different angle ψ_i, see Fig. 2(a) .The experimental observations suggest a simplification for the polarizing filter array due to the π phase shift obtained; thus, it is not necessary to use all linear polarizing filters for all patterns. For example, in the case of four steps, we only need to place two polarizers (P_0 and P_1), each one covering two patterns with complementary phase shifts; then, $\psi_0 = 0$ deg and $\psi_1 = 46.557$ deg,[2] which leads to phase shifts ξ of 0, 0, $\pi/2$, π, and $3\pi/2$, and can be seen in Fig. 2(b), with the dotted boxes representing the polarizing filters. This result allows us to know the phase profile. Since n-interferograms can be obtained simultaneously, the dynamic study of a phase objects can be carried out.

3.4 *Phase Objects*

If placed on B arm of the interferometer, a transparent object (without absorption) can be expressed as:

$$O(x,y) = e^{i\cdot\phi(x,y)}, \tag{13}$$

where $\phi(x,y)$ is a real function; this object is known as a phase object. Consider the special case where $|\phi(x,y)|^2 \ll 1$, resulting in the kind of transparent objects known as thin phase objects we obtain

$$O(x,y) = 1 + i\cdot\phi(x,y); \tag{14}$$

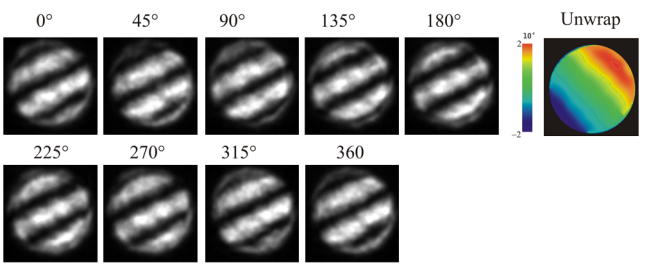

(a) (b)

Fig. 6 Tilted wavefront. (a) Nine 45 deg phase-shifted interferograms and (b) unwrapped phase data map.

with i being a constant, maintaining a constant phase relationship $\pi/2$ because $i = e^{i\cdot\pi/2}$. Equation (4) allows us to retrieve the phase profile of the transparent sample. The phase reconstruction is performed using Eqs. (11) or (12), according to the case.

4 Experimental Results: Static and Dynamic Distributions

The phase gratings that were used are the commercially available ones. (Edmund Optics' transmission grating, dimensions: 25×25 mm; dimensional tolerance: ± 0.5 mm; substrate: Optical Crown Glass). The monochromatic camera used is based on a CMOS sensor with 1280×1024 pixels and with a pixel pitch of $6.7\,\mu$m. Each interferogram was typically composed of arrays of 600×512 pixels, and filtered with a conventional low-pass filter to remove sharp edges and detail from the image, leaving smooth gradients and low-frequency detail. To reduce differences of irradiance and fringe modulation, each interferogram used was subjected to a rescaling and normalized process. This procedure generates patterns of equal background and equal fringe modulation. There are several two-dimensional (2-D) phase unwrapping algorithms; however, for simplicity, the method used for unwrapping the phase data was a non-iterative fast cosine method.[12]

4.1 *Static Distributions: Four Interferograms Case*

A phase dot generated with a magnesium fluoride film (MgF_2) on a glass substrate, was placed in the path of beam B, while beam A was used as a reference; the results obtained are shown in Fig. 3. Figure 3(a) shows the four patterns with $\pi/2$ phase shifts obtained in a single shot, and Fig. 3(b) presents the phase profile of the object, in false color coding. More than four interferograms could be used, whether for N-steps phase-shifting interferometry or for averaging images with the same shift. Figure 4 presents the comparative case, between the measurements of the phase dot, measured with a two window interferometer with the measurement made with the proposed system. Figure 4(a) shows cross sections along the axis x, and Fig. 4(b) shows cross sections along the axis y. Variations which increase near the edges can be observed between the two measures, and are due to processing of the interferograms. The results presented in Ref. 1 show the interferograms were not filtering as evidenced by speckle noise, which leads to errors in the unwrapped phase. This can be seen on the graph of the differences along the two directions in Fig. 4(c).

The difference presented in the results obtained, which were compared with Ref. 1, is caused mostly by object deterioration. In the results presented, the fringe patterns obtained correspond to changes in the curvature surface.

Comparatively, the results obtained with the proposed optical system are equal to those obtained with an interferometer double-fixed window, however, the implementation of this optical system becomes simpler since it is easier to place the necessary components. Also, we are able to use phase grids with other periods, or absorption grids, only taking in consideration the correct separation of the two windows.

The accuracy in measurements is the one typical of phase-shifting. Some trade-offs appear while placing several images over the same detector field, but for low frequencies interferograms (with respect to the inverse of the pixel spacing) the influence of these factors seems to be rather small if noticeable.

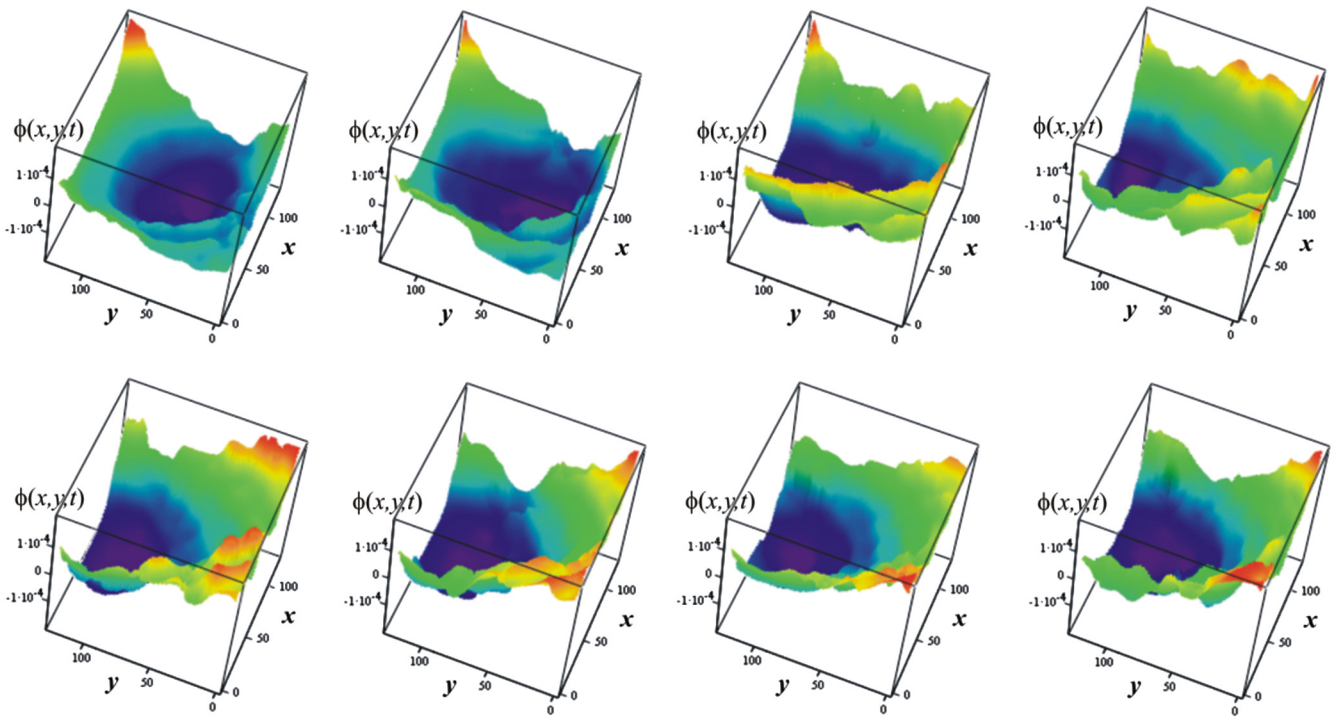

Fig. 7 Dynamics distributions; representative frames; evolution of the phase profile, one capture per 2 sec (Video 1, QuickTime, MOV, 725 KB) [URL: http://dx.doi.org/10.1117/1.OE.51.5.055601.1].

4.2 *Static Distributions: Case of Nine Interferograms*

To demonstrate the use of several interferograms, we choose the symmetrical $n = (N + 1)$ phase steps algorithms,[7] for data processing (case $N = 8$). A constant phase shift value of $2\pi/N$ is employed when using these techniques. The phase shifts of π due to the grid spectra allow the use of a number of polarizing filters that is less than the number of interferograms, simplifying the filter array (see Fig. 5). According to Fig. 5(b), it can be shown that for a symmetrical nine, $\psi_1 = 0$, $\psi_2 = 92.989$, $\psi_3 = 22.975$, $\psi_4 = 46.577$, and $\psi_5 = 157.903$ deg. In this case, each resulting step ξ corresponds to a 45-deg phase-shift.[2] The corresponding results and calculated phases are shown in Fig. 6. The experimental results show the interference pattern and unwrapped phase generated by a tilted wavefront. This system is capable of obtaining $n = N + 1$ interferograms in a single capture.

4.3 *Dynamic Distributions*

A dynamic phase object is shown in Fig. 7 (Video 1). It corresponds to flowing oil on a glass microscope slide allowing to flow under the effect of gravity. The phase object was put in front of B windows of the system of Fig. 1. For this case, four interferograms are used to process the optical phase.

The figure shows the temporal evolution of the oil flow (Video 1). The oil drop is deformed due to the action of gravity during the observation period. With better control of the parameters of the experiment we can calculate the fluid velocity, and that is a future work of the techniques presented. One of the advantages of phase-shift systems is that they allow simultaneous observation of dynamic events.

5 Conclusions

The experimental set-up for an adjustable two-window interferometer based in a Mach Zehnder configuration has been described to obtain the phase profile of phase objects from the analysis of optical phase using polarizing phase shifting techniques. This system is able to obtain N interferograms with only one shot ($n \leq 16$).

Tests with four phase-shifts were presented, but we also tested other approaches using different phase-shifts attained by using linear polarizers with their transmission axes at the proper angle before detection (case of nine interferograms). The phase shifts of π due to the grid spectra allows the use of a number of polarizing filters which is less than the number of interferograms, simplifying the filter array. The interferometric system allows the analysis of static objects and dynamics objects.

Acknowledgments

The authors are very grateful for the funding support granted by The Tecnological University of Tulancingo (http://www.utec-tgo.edu.mx/fotonica.html). Authors thank M. A. Ruiz for his contribution in proofreading the manuscript. The experimental results are part of the bilateral projects between Mexico-Chile (CONACYT-CONICYT) and Mexico-Italy (CONACYT-MAE). Author D.-I. Serrano-García (Grant: 227470/31458) is very grateful to CONACYT for the graduate scholarship granted, and expresses sincere appreciation to Geliztle. Author N.-I. Toto-Arellano expresses sincere appreciation to *Luisa*, *Miguel*, and *Damian* for the support provided, and to Sistema Nacional de Investigadores (SNI) for grant 47446. Partial support from CONACYT and Vicerrectoría de Investigación y Estudios de Posgrado (VIEP) through projects 124145 and 154984 is also acknowledged.

References

1. N.-I. Toto-Arellano et al., "Phase shifts in the Fourier spectra of phase gratings and phase grids: An application for one-shot phase-shifting interferometry," *Opt. Express* **16**(23), 19330–19341 (2008).
2. G. Rodriguez-Zurita et al., "One-shot phase-shifting interferometry: Five, seven, and nine interferograms," *Opt. Lett.* **33**(23), 2788–2790 (2008).
3. G. Rodriguez-Zurita et al., "One-shot phase-shifting phase-grating interferometry with modulation of polarization: case of four interferograms," *Opt. Exp.* **16**(11), 7806–7817 (2008).
4. N. I. Toto-Arellano et al., "Slope measurement of a phase object using a polarizing phase-shifting high-frequency Ronchi grating interferometer," *Appl. Opt.* **49**(33), 6402–6408 (2010).
5. D. I. Serrano-García et al., "Simultaneous phase-shifting cyclic interferometer for generation of lateral and radial shear," *Rev. Mex. Fís.* **57**(3), 255–258 (2011).
6. B. Barrientos-García et al., "Spatial phase-stepped interferometry using a holographic optical element," *Opt. Eng.* **38**(12), 2069–2074 (1999).
7. D. Malacara, M. Servin, and Z. Malacara, "Phase detection algorithms," Chapter 6, in *Interferogram Analysis for Optical Testing*, 2nd Ed. CRC Press (24 March 2005).
8. M. Novak et al., "Analysis of a micropolarizer array-based simultaneous phase-shifting interferometer," *Appl. Opt.* **44**(32), 6861–6868 (2005).
9. J. C. Wyant, "Dynamic Interferometry," *Optic. Photon. News* **14**(4), 36–41 (2003).
10. Q. Kemao, W. Xiaoping, and A. Asundi, "Grating-based real-time polarization phase-shifting interferometry: error analysis," *Appl. Opt.* **41**(13), 2448–2453 (2002).
11. J. E. Miller and N. J. Brock, "Methods and apparatus for splitting, imaging, and measuring wavefronts in interferometry," U.S. Patent No. 2003/0053071 A1 (2003).
12. C. Ghiglia and M. D. Pritt, *Two-Dimensional Phase Unwrapping: Theory, Algorithms, and Software*, Wiley, New York (1998).

David-Ignacio Serrano-García received his BS degree in 2008 from Tecnológico de Monterrey, Campus Monterrey in México and his MSc degree in optical sciences at Centro de Investigaciones en Óptica (CIO), México in 2010. Now he is working toward his PhD in optical sciences at the same institution. He has been an active SPIE and OSA student member since 2006 and his research interests include optical metrology, polarization phase shifting interferometry, and digital image processing. In 2011, he received a SPIE Scholarship for his potential contributions to the field of optics, photonics, or related fields.

Noel-Ivan Toto-Arellano received his BS degree in physical sciences at Universidad Veracruzana, México, his MSc in optical sciences from Benemerita Universidad de Puebla (Puebla, México, 2005), and his PhD in optical sciences by the same institution (2008). He did two post-doctoral internships at CIO (León, Gto. México, 2009 to 2011). He currently holds a research professor position in Universidad Tecnológica de Tulancingo, Hidalgo, México, supporting the creation of a photonics engineering program at the same university. He has authored 15 articles in interferometry and Fourier optics, five book chapters, and two handbooks. He holds three national science and technology awards and two medals for innovations granted by the Mexican Institute of Industrial Property. His current research

interest include physical optics, interferometry, laser applications, image formation (spatial filtering, holography and tomography), Fourier optics, and optical metrology using moiré and speckle interferometry, contouring for structured light projection.

Amalia Martinez-Garcia received her BS degree in physics from Facultad de Ciencias Físico-Matemáticas, UANL, Monterrey, her MS degree from the Division of Applied Physics, CICESE, Ensenada, and her PhD in Optics at CIO, León, Mexico. From 1987 to 1996, she was a research scientist at CICESE. She held a sabbatical position at CIO during 1995 and 1996. Currently, she is researcher at CIO, a national researcher for the National System of Researchers, Mexico, a member of the Mexican Academy of Optics and SPIE. She is the executive secretary of the Mexican Academy of Optics in 2011 and 2012. Her research interests are optical metrology with holography, speckle and moiré techniques, images correlation and stereo vision systems.

Juan-Antonio Rayas-Álvarez received his BS degree in industrial engineering from Universidad Tecnológica del Norte de Guanajuato in 2002. He currently holds a research technician position at Centro de Investigaciones en Óptica A.C. (CIO) in León, Gto. México, since 1999. His research interests are optical metrology using moiré and speckle interferometry techniques, contouring techniques using structured light projection (laser and white light), digital image and fringes processing, and photoresist deposition techniques.

Gustavo Rodriguez-Zurita received his BS degree from the Universidad Veracruzana in 1977 (Physics), his MS degree in optics from INAOE (Puebla, 1978) and his doctor degree from the Friedrich-Schiller-Universität of Jena (Germany, 1990). He is co-founder of the Centro de Investigaciones en Optica (CIO-León, 1978 to 1982). He then joined the Benemerita Universidad Autonoma de Puebla until today, teaching physics and optics at both undergraduate and graduate levels as a member of the Facultad de Ciencias Fisico-Matematicas. He has authored more than 55 papers on optical interferometry and Fourier optics. His current research interests include physical optics, interferometry, laser applications, image formation (spatial filtering, holography and tomography) and Fourier optics.

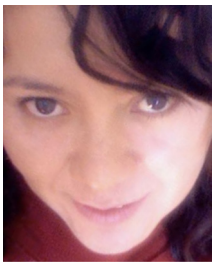

Areli Montes-Pérez received her BS degree in physical sciences from Benemérita Universidad Autónoma de Puebla (BUAP), México, her MSc in optical sciences (Puebla, México, 2006) and her PhD. In optical sciences from the same institution (Puebla, México, 2010). She currently holds a researcher professor position in The Optical Physics Laboratory of BUAP, México (2010 to current). She has authored 5 articles in Optical Tomography, Interferometry and Fourier Optics, 1 Books Chapters, and has participation in 28 national and 6 international conferences. Her current research interest fields include Optics and Photonics, Interferometry, Laser Applications, Spatial Filtering, Tomography using Hilbert Transforms.